Clays and Clay Minerals, Vol. 58, No. 3, 327–339, 2010.

USE OF NATURAL AND MODIFIED MAGADIITE AS ADSORBENTS TO REMOVE Th(IV), U(VI), AND Eu(III) FROM AQUEOUS MEDIA – THERMODYNAMIC AND EQUILIBRIUM STUDY

DENIS L. GUERRA[1,*], JOSANE N. FERRREIRA[1], MÁRIO J. PEREIRA[1], RÚBIA R. VIANA[1], AND CLAUDIO AIROLDI[2]

[1] Universidade Federal de Mato Grosso, UFMT, Centro de Recursos Minerais, Cuiabá, Mato Grosso 78060 900, Brazil
[2] Chemistry Institute, State University of Campinas, P. O. Box 6154, 13084-971 Campinas, São Paulo, Brazil

Abstract—The contamination of aquatic environments by toxic metals such as radionuclides is of great concern because of the tendency of those metals to accumulate in the vital organs of humans and animals, causing severe health problems. The objective of this study was to investigate the use of natural and modified magadiite clay as an adsorbent to remove Th(IV), U(VI), and Eu(III) from aqueous solutions. Magadiite from the Amazon region, Brazil, was modified chemically with 5-mercapto-1-methyltetrazole (MTTZ) using a multi-step or heterogeneous synthesis pathway. The natural and modified materials were characterized using ^{29}Si and ^{13}C nuclear magnetic resonance, scanning electron microscopy, nitrogen gas adsorption, and elemental analysis. The physical-chemical properties of the chemically modified magadiite sample were modified, *e.g.* the specific surface area changed from 35.0 to 678.9 $m^2\ g^{-1}$. The ability of the magadiite to remove Th(IV), U(VI), and Eu(III) from aqueous solution was then tested by a series of adsorption isotherms adjusted to a Sips equation. The effects of properties such as pH, contact time, and metal concentration on the adsorption capacity were studied. The adsorption maxima were determined to be 7.5×10^{-3}, 9.8×10^{-3}, and 12.9×10^{-3} mmol g^{-1} for Th(IV), U(VI), and Eu(III), respectively. From calorimetric determinations, the quantitative thermal effects for all these cations/basic center interactions gave exothermic enthalpy, negative Gibbs free energy, and positive entropy, confirming the energetically favorable conditions of such interactions at the solid/liquid interface for all systems.

Key Words—Calorimetry, Chemical Synthesis, Interfaces, Magadiite, Surface Properties, Thermodynamic Properties.

INTRODUCTION

Magadiite clay is generated from soils and sedimentary deposits through weathering, diagenesis, and hydrothermal effects. This process involves degradation and transformation of precursor silicates, including precipitation from solution. Naturally occurring magadiite is found, but rarely, in the Amazon region because the Amazon climate is normally warm-humid, causing acidic lixiviation in soils, conditions that are unfavorable for the formation of the lamellar structure (Almond *et al.*, 1997; Guo *et al.*, 2004; Shahwan and Erten, 2005; Guerra *et al.*, 2007; Beurlen *et al.*, 2008; Guerra *et al.*, 2008a). Magadiite, with the ideal formula $Na_2Si_{14}O_{29}.nH_2O$, is a platy, hydrous sodium silicate, which is composed of one or multiple negatively charged sheets of SiO_4 tetrahedra with abundant silanol-terminated surfaces (Almond *et al.*, 1997; Komori *et al.*, 2000; Mizukami *et al.*, 2002; Guo *et al.*, 2004). Physical properties include a large capacity for ion exchange where Na^+ ions can be replaced by protons, other cations, or large quaternary ammonium ions (Almond *et al.*, 1997; Garces *et al.*, 1988).

Meeting the stringent coolant-purity requirements of the nuclear industry is solely attributable to inorganic ion exchangers. In recent years, clays, layered materials, and zeolites have been used extensively in the chemical decontamination process for radionuclide recovery, regeneration of decontaminants, and removal of the formulation chemicals from the coolant (Leppert, 1990; Almond *et al.*, 1997; Ruiz and Airoldi, 2004; Lazarin and Airoldi, 2007; Macedo *et al.*, 2007; Xiu-Wen *et al.*, 2007; Tang *et al.*, 2009).

Magadiite exhibits a variety of properties, such as sorption of water and polar organic molecules (Guo *et al.*, 2004). Magadiite is used as an adsorbent of toxic metals not only because of its ability to immobilize the toxins, but also because it is relatively simple in comparison to organic polymers, with faster metal ion-exchange kinetics, good swelling resistance in different solvents, and chemical stability (Macedo *et al.*, 2007). The present study reports the use of original and modified magadiite as adsorbents to extract the toxic metals commonly present in waters from a variety of sources and in industrial effluents. For this purpose, the adsorption isotherms of Th(IV), U(VI), and Eu(III) from aqueous medium at room temperature were explored, bearing in mind the influence of different parameters such as pH, radionuclide concentration, and contact time. The ability of natural and modified magadiite to remove the radionuclide ions was investigated using a

* E-mail address of corresponding author:
denis@cpd.ufmt.br
DOI: 10.1346/CCMN.2010.0580304

batch-adsorption procedure. The chemical modification process was developed by means of functionalization of Amazon magadiite clay using 5-mercapto-1-methyltetrazole *via* a multi-step, heterogeneous synthesis pathway (Prado and Airoldi, 2001). The quick adsorption process reached equilibrium before 2, 3, and 4 h for Eu(III), U(VI), and Th(IV), respectively, with adsorption maxima at pH 4.0. The energetic effect caused by radionuclide/phyllosilicate surface interaction at the solid/liquid interface was determined through the calorimetric titration procedure.

EXPERIMENTAL METHODS

Reagents and raw material

3-chloropropyltriethoxysilane 95% (CPTS) (M_w = 240.810 and d = 1.007 g cm^{-3}), triethylamine 98% (TEA) (M_w = 101.191 and d = 0.726 g cm^{-3}), and 5-mercapto-1-methyltetrazole 98% (MTTZ) (M_w = 116.151 and d = 1.002 g cm^{-3}) were purchased from Sigma-Aldrich. Doubly distilled deionized water (DDW) was used in the preparation of the solutions, wherever required. Solutions of uranyl were prepared from a suitable reagent-grade nitrate salt by dissolving it in DDW.

The magadiite sample used here was obtained from Nhamundá area, State of Amazonas, in the Amazon region in northern Brazil. The <2 μm size fraction was separated by sedimentation. The cation-exchange capacity (CEC) was measured using ammonium acetate at concentrations of 2.0 mol dm^{-3} at pH 8.0, in order to evaluate the potential use of Amazon magadiite for intercalation. The result obtained was 78.0 meq/100 g of clay (M) on an air-dried basis. The magadiite sample, with a particle size which would pass through a 70−230 mesh, was activated in a stream of dry nitrogen by heating at 423±1 K for 12 h and used immediately.

Chemical modification of the clay

The MTTZ (20.0 g, 215 mmol) was immersed in hexane (100.0 cm^3); 3-chloropropyltriethoxysilane (95%) (CPTS) and triethylamine (TEA) were then added in a 1:2:1 stoichiometry (MTTZ:CPTS:TEA) (Figure 1). The mixture was heated for 48 h at 338±1 K with magnetic stirring under a nitrogen atmosphere using standard Schelenk-tube techniques. The mixture was filtered to eliminate the triethylamine chloride precipitate. The hexane was evaporated and the excess CPTS was distilled under vacuum (423±1 K and 0.75 Hg) (Pérez-Quintanilla *et al.*, 2006, 2007). The MTTZ derivative (50.0 cm^3) was reacted with a natural clay sample (M) (25.0 g) (5 h at 435±1 K under high vacuum) in dry toluene (200.0 cm^3) with mechanical stirring (48 h under reflux conditions with nitrogen atmosphere). The resulting modified clay sample (M_{MTTZ}) was filtered and washed with toluene (2×100.0 dm^3), ethanol (2×100.0 dm^3), and diethyl ether (2×100.0 dm^3). Finally, the product was heated for 4 h at 385±1 K under vacuum (Pérez-Quintanilla *et al.*, 2006, 2007).

Characterization methods

The X-ray diffraction (XRD) patterns of the original Na-magadiite and organoclay were recorded from random mounts using a Rikagu D-Max 2200 Powder Diffractometer with CuKα (0.154 nm) radiation in the region between 2 and 50º2θ at a speed of 2º2θ min^{-1}, a step size of 0.050º2θ, and Ni filter.

Nuclear magnetic resonance spectra of the samples were obtained using a Bruker AC 300/P spectrometer at room temperature. For each run, ~1 g of each solid sample was compacted into a 7 mm zirconium oxide rotor. The measurements were obtained at frequencies of 59.63 and 75.47 MHz for silicon and carbon atoms, respectively, with a magic angle spinning of 4.00 kHz. In order to increase the signal to noise ratio of the solid-state spectra, the CP/MAS technique was used. ^{29}Si and ^{13}C CP/MAS spectra were obtained with pulse repetitions of 3 s for both nuclei and contact times of 1 and 3 ms, respectively.

The elemental analysis (wt.% C, N, and S) was determined using a Perkin-Elmer 2400 Series II micro-elemental analyzer, and at least two independent determinations were performed for modified clay samples.

The Brunauer-Emmett-Teller (BET) surface area, pore diameter, and pore volume were obtained from nitrogen adsorption/desorption in a Micromeritics ASAP 2000 BET surface analyzer system (Brunauer *et al.*, 1938). The mesopore-size distribution was obtained by applying the Barret-Joyner-Halenda (BJH) method to the adsorption branch of the isotherm (Barret *et al.*, 1951).

The scanning electron microscopy (SEM) study of the powdered samples was obtained using an SM 6360LV instrument, under vacuum, accelerated at 20 kV (Shahwan and Erten, 2005).

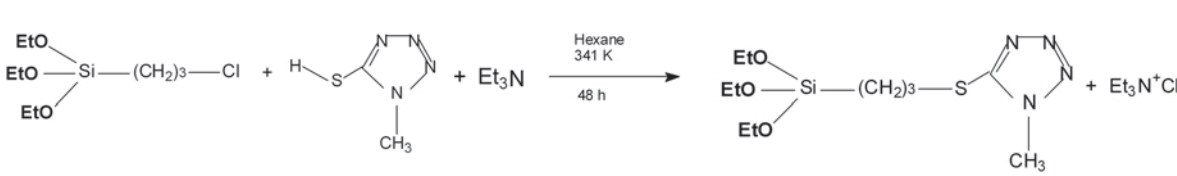

Figure 1. Synthesis of MTTZ derivative.

A simple and sensitive spectrophotometric method based on colored complexes, Arsenazo III with U(VI) and Th(IV) and Alizarin Red S with Eu(III) in aqueous medium, was used for radionuclide determination. The concentrations of metal ions in the supernatant were determined using a Systronic-117 UV-vis spectrophotometer, by measuring absorbance at λ_{max} of 660 nm for Th(IV), 652 nm for U(VI), and 531 nm for Eu(III) (Sharma and Tomar, 2008). For each experimental point, the reproducibility was checked by at least one duplicate run.

The thermal effects of metal cations interacting with original and modified magadiite samples were assessed by calorimetric titration using an isothermal calorimeter, Model LKB 2277, from Thermometric (Jarfalla, Sweden). In this titration, the metallic solution was added to a suspension of ~20 mg of each sample in 2.0 cm^3 of water, under stirring at 298±1 K.

Adsorption

The adsorption experiments were performed batch-wise by suspending a series of 20 mg samples of the solid in 20.0 cm^3 aqueous solutions of cations at concentrations varying from 1.25×10^{-2} to 2.50×10^{-2} mmol dm^{-3}, under orbital stirring for 24 h at 298±1 K. Profiles of the adsorption isotherms obtained represented by the number of moles adsorbed (N_f) (Prado and Airoldi, 2001; Malkoc *et al.*, 2006; Alcântara *et al.*, 2007; Sheng *et al.*, 2008; Cestari *et al.*, 2009) *vs.* the number of moles at equilibrium per volume of solution (C_S), for a series of isotherms, revealed that the adsorption process conforms to the Sips (1948) model which combined the Langmuir (1918) and Freundlich (1906) equations (equation 1). The Sips isotherm is a three-parameter fitting equation and combines the features of both the Freundlich and Langmuir models. The Sips isotherm model will give a Langmuir isotherm model when $n = 1$.

$$N_f = \frac{N_S K_S C_S^{1/n}}{1 + K_S C_S^{1/n}} \quad (1)$$

Where C_s is the concentration of solution at equilibrium (mol dm^{-3}), N_f and N_S are the concentrations of metal adsorbed and the maximum amount of metal adsorbed per gram of clay (mol g^{-1}), respectively, which depend on the number of available adsorption reactive sites, K_S is the equilibrium constant, and n is the Freundlich exponent (Sips, 1948). Firstly, the effect of pH on adsorption for all clay samples was evaluated by varying this parameter over the range 1.0−5.0, with addition of 0.10 mol dm^{-3} of nitric acid or sodium hydroxide. The pH of the solutions was measured using a pH/Ion Analyzer, model 450 M (Analyzer, São Paulo, Brazil). In the investigation of the influence of contact time in the adsorption process, the kinetic parameters were analyzed by the Lagergren pseudo-second-order model (Lagergren, 1898).

The thermodynamic, Lagergren pseudo-second-order, and Sips models were fitted using the non-linear fitting routines of the software *Microcal Origin* 7.0. A correlation coefficient (r^2) and a probability value ($p = 0.0001$) represent the 'goodness of fit.' In addition, the model was also evaluated by average relative error function (equation 2), which measures the differences in the amount of the metallic cation taken up by the adsorbent predicted by the models and the actual N_f measured experimentally (Babel and Kurniawan, 2003).

$$F_{ERROR}(\%) = 100x\sqrt{\sum_i^p \left(\frac{N_f i\text{model} - N_f i\text{experimental}}{N_f i\text{experimental}}\right)^2 \left(\frac{1}{p-1}\right)} \quad (2)$$

RESULTS AND DISCUSSION

Characterization of materials

Different experiments were performed using bridged organosilane MTTZ (5-mercapto-1-methyltetrazole) as an intercalating agent to synthesize inorganic-organic hybrid layered material. In the modified magadiite structure, the organic links present in the initial organosilane could be incorporated into the interlayer space of layered silicates, covalently bonded to the surfaces of magadiite-type inorganic layers. Indeed, XRD patterns of natural and modified magadiite (Figure 2a,b) exhibit 001 reflections corresponding, in the case of original Na-magadiite, to a basal spacing of 1.580 nm due to the presence of Na^+ cations and water molecules present between the magadiite layers, the thickness of which is ~0.950 nm (Almond *et al.*, 1997; Díaz *et al.*, 2007) (Figure 2a), whereas, after the chemical modification process, the basal spacing increased to 3.220 nm because of the effective intercalation of the MTTZ molecules in the interlayer space (Figure 2b). Taking into account the thickness (0.950 nm) of the Na-magadiite layers, the space occupied by the bridged polysiloxane corresponds to 2.27 nm, confirming that the organic-inorganic precursor was successfully intercalated into the interlayer space with the MTTZ units oriented perpendicular to the phyllosilicate layer. The great influence of the number of MTTZ ions on the surface and on the constitution and distribution of the ions has been reported previously (Pérez-Quintanilla *et al.*, 2007). The mass fraction of intercalated phyllosilicate can be estimated as the relative intensities of the reflection originating from the 'unchanged' and the 'expanded' layers. In the intercalated sample, the degree of intercalation reaction could be estimated as 88.03%, indicating that the MTTZ molecules are arranged in monolayers between the phyllosilicate layers (Pérez-Quintanilla *et al.*, 2007).

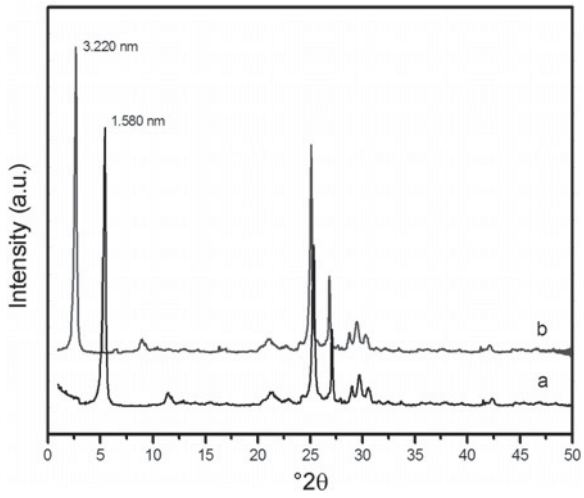

Figure 2. Powder XRD patterns of natural (a) and modified (b) magadiite.

Nuclear magnetic resonance in the solid state (solid-state NMR) is a technique which gives valuable information about the bonding of the pendant chains anchored on an inorganic backbone. For this purpose, silicon and carbon nuclei were observed in order to better characterize the synthetic compound. Through the distribution of groups containing silicon atoms on the surface, the inorganic framework of the matrices and the intercalated species can be understood (Almond *et al.*, 1997). For the natural magadiite spectrum a Q^3 signal at −99.2 ppm was observed (Figure 3a), which was related to the stoichiometry of the silicate. Strongly hydrogen-bonded water molecules gave a broad peak. On the other hand, one peak with a Q^4 signal was observed in magadiite samples at −109.6. Each magadiite layer contained equal numbers of Na^+ cations or protons to counter the negative charge on the oxygen atoms, being neutral structures. The spectrum of the functionalized magadiite showed a marked decrease in the intensity of the Q^3 signal, verifying the anchoring of the functional groups to Si-OH (Figure 3b). In addition, two new peaks at −52.5 and −77.1 ppm were assigned to the T^2 $[(SiO)_2SiOH{-}R]$ and T^3 $[(SiO)_3Si{-}R]$ sites, respectively (Pérez-Quintanilla *et al.*, 2007).

For carbon, the spectrum shown in Figure 3c provides information about the polysiloxane framework such as various local environments of the atoms involved and the attachment of pendant groups, and in the present case the assignments were based on a previously studied analogous system (Pérez-Quintanilla *et al.*, 2007). The three carbon atoms related to the ligand ring, numbered 3, 4, and 5, gave signals at 10.0, 19.2, and 24.3 ppm, respectively. The signal due to methylene 2 of the ethoxy group appears at 48.2 ppm and the signal from the methyl group is at 21.1 ppm. The aromatic carbon labeled 6 was assigned to the signal at 135.2 ppm. Finally, the signal due to the methyl in the heterocycle numbered 7 appears at 22.2 ppm. These results prove that the preparation of the new material was successful and confirm the results of previous studies (Pérez-Quintanilla *et al.*, 2006, 2007; Evangelista *et al.*, 2007; Cestari *et al.*, 2009).

The quantity of molecules (L_0) attached to the magadiite surface was calculated from the percentage of sulfur in the chemically modified clay sample, as estimated by elemental analysis, using equation 3 (Dias Filho, 1998; Pérez-Quintanilla *et al.*, 2006):

$$L_0 = \frac{\%S \times 10}{\text{sulfur atomic weight}} \quad (3)$$

The C/S molar ratio calculated from the elemental analysis of M_{MTTZ} indicates a 1:1 stoichiometry between the silanol groups on the clay surface and the ligand. Taking into account L_0 and the specific surface area (SA_{BET}) of modified magadiite, the average surface density, d, of the attached molecules and the average intermolecular distance, I, can be calculated by applying equations 4 and 5 (Dias Filho, 1998; Pérez-Quintanilla *et al.*, 2006):

$$d = N_A \frac{L_0}{SA_{BET}} \quad (4)$$

$$I = \left(\frac{1}{d}\right)^{1/2} \quad (5)$$

where N_A is Avogadro's number. The results obtained confirm a high efficiency in the chemical modification of natural Na-magadiite. The large degree of functionalization obtained with the M_{MTTZ} can, therefore, be explained as a consequence of its large surface area (Table 1).

The BET surface areas of the natural and modified clay samples demonstrated that chemical modification caused the formation of micropores in the solid particles, resulting in a greater surface area: 678.8 $m^2\ g^{-1}$ for M_{MTTZ} and 35.0 $m^2\ g^{-1}$ for the natural M sample. The pore diameters change in the same direction, varying from 1.4 nm for the natural to 4.8 nm for the anchored clay. The textural analyses of natural and modified magadiite samples (Table 1) revealed that the textures depend on particle size, shape, and distribution of cracks and pores in the material, and, therefore, cannot be represented as a general characteristic of the particular type of material. The modified sample gave a unimodal distribution of pore sizes while M showed a bimodal distribution (Figure 4a). The adsorption-desorption isotherms of gaseous nitrogen of the natural and modified magadiite are type IV according to the I.U.P.A.C (Pérez-Quintanilla *et al.*, 2008; Jänchen *et al.*, 2009) classification and have a H1 hysteresis loop that is representative of materials with pores of constant cross-section size. The volume adsorbed for all isotherms at a relative pressure (P/P_0) of ~0.5 represents capillary condensation

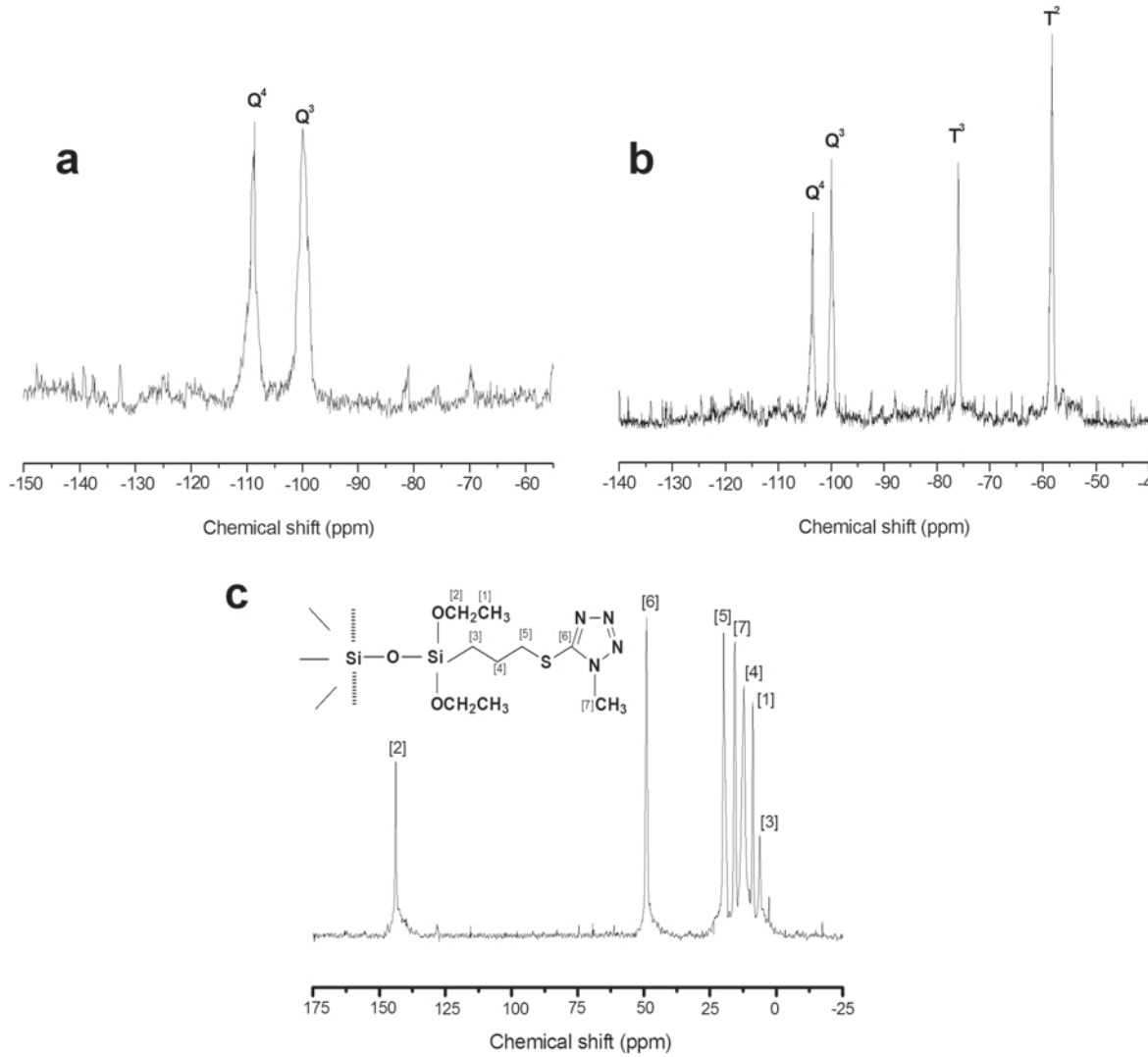

Figure 3. ^{29}Si MAS NMR spectra of natural (a) and modified (b) magadiite and ^{13}C MAS NMR spectrum of modified magadiite (c).

of nitrogen within the uniform mesopore structure (Figure 4b). The results are in accord with findings by Shanmugharaj *et al.* (2006) who found that the intercalation of trifunctional silane in smectites tended to be more successful in aqueous media than in ethylene glycol.

Table 1. Textural properties of magadiite samples and quantification of organic molecules anchored in the modified magadiite samples.

Sample	Surface area-SA_{BET} (m^2 g^{-1})	Micropore area (m^2g^{-1})	Pore diameter (nm)	Pore volume (cm^3g^{-1})	L_0 (mmol g^{-1})	d (molecules nm^{-2})	I (nm)
M	35.0	10.0	1.4	0.1	–	–	–
M_{MTTZ}	678.8	37.1	4.8	0.3	1.12±0.1	0.83±0.1	1.01±0.1

L_0: quantity of adsorbed molecules.
d: average surface density of adsorbed organic molecules.
I: intermolecular distance.

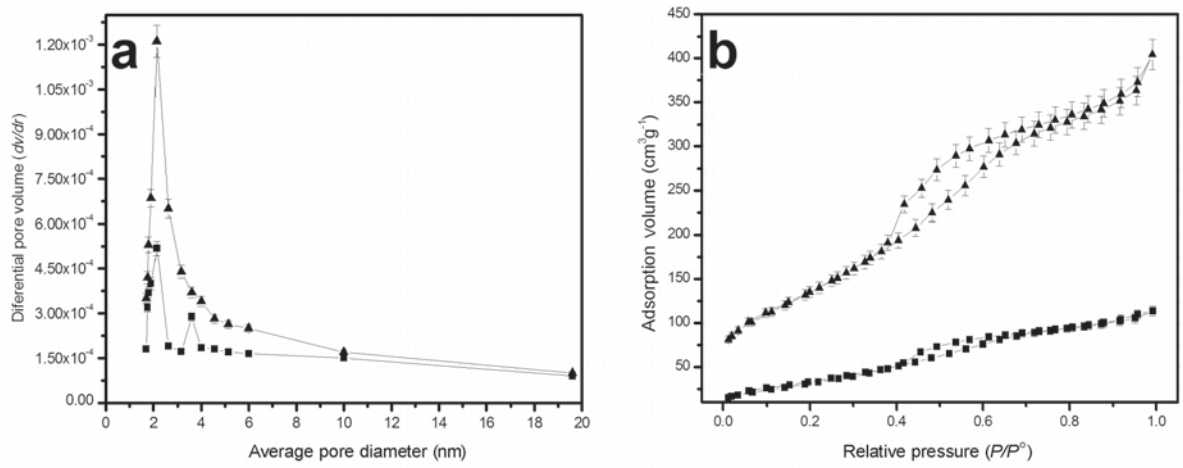

Figure 4. Pore distribution of natural and modified magadiite samples obtained by the BJH method (a) and nitrogen adsorption-desorption isotherms of natural and modified magadiite samples obtained by the BET method (b) (■ – M; ▲ – M_{MTTZ}).

Scanning electron microscopy images of the phyllosilicate samples were used only to verify the presence of macropores in the structure of the matrices (Figure 5a,b) because micro- and mesopore structures could not be observed at the magnification used in these experiments. A foliated structure of the phyllosilicates was observed, with some fissures and holes, indicating the presence of a macroporous structure. The fissures and holes probably contribute somewhat to the diffusion of the radionuclide to the phyllosilicate adsorbent surfaces. The number of macroporous structures was confirmed by the large specific surface areas of the modified phyllosilicate (Table 1). The presence of agglomerated particles of nanodimensions was also noted in the natural magadiite samples. Twinned edges and well defined angles were also observed. Small aggregates of rounded crystal coexisted with regular magadiite particles with particle size mostly <5.0 μm (Guerra *et al.*, 2006). The major contribution of the radionuclide uptake can, therefore, be attributed to micro- and mesoporous structures.

Effect of pH

The extractability of the cations from the solution phase is pH dependent. The pH of the aqueous solution, which increased almost linearly from pH 4.0, is an important controlling parameter in the adsorption process. Both the extent of adsorption and the amount adsorbed (N_f) showed positive changes (Figure 6a,b). The effectiveness of the process can be expressed by a plot of the number of moles adsorbed (mmol g^{-1}) *vs.* pH for the cations involved. From the corresponding data for each metal, an increase in pH was followed by an increase in adsorption, reaching the maximum capacity at pH 4.0. For greater pH values a slight decrease in adsorption for Th(IV), U(VI), and Eu(III) was observed. The observed reduction in the level of metal-ion removal

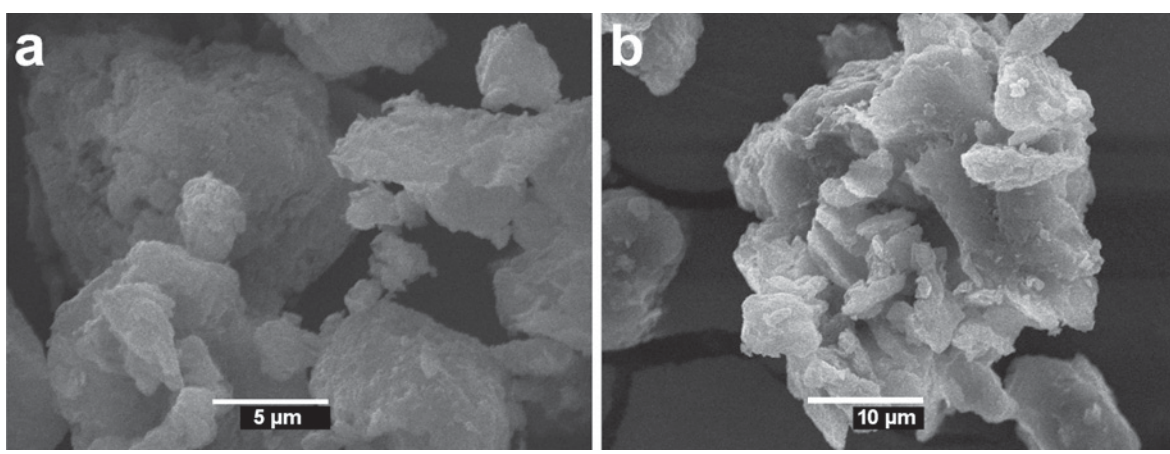

Figure 5. SEM images of natural (a) and chemically modified (b) magadiite samples.

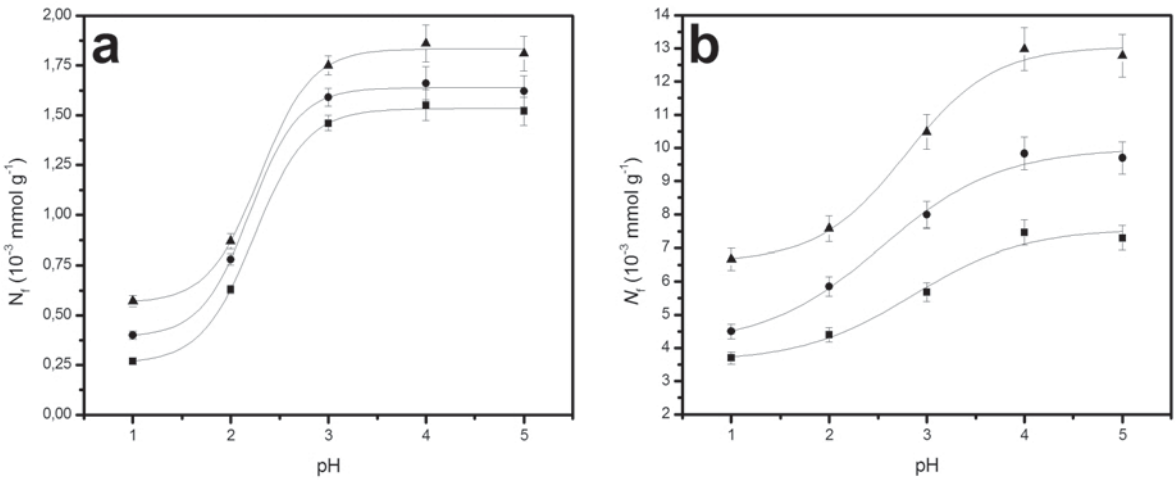

Figure 6. Effect of pH on the adsorption of cations onto natural (a) and modified (b) magadiite samples from aqueous solution [■ – Th(IV), ● – U(VI), and ▲ – Eu(III)] (clay 1.0 g dm^{-3}, time 8.0 h, and controlled temperature – 298±1 K).

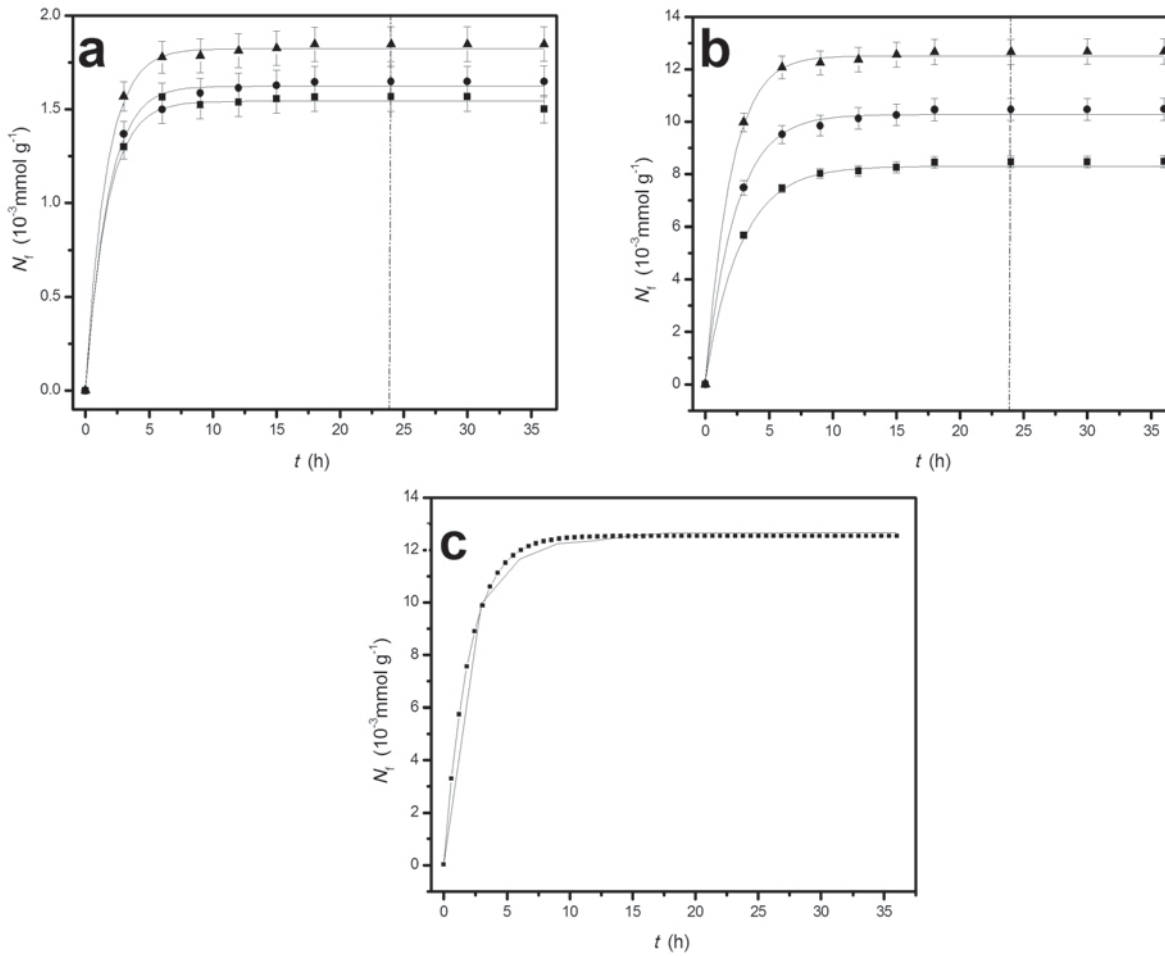

Figure 7. Effect of contact time on the adsorption onto natural (a) and modified magadiite (b) samples [■ – Th(IV), ● – U(VI), and ▲ – Eu(III)] and example of curve obtained by non-linear regression: M_{MTTZ}/Eu(III) (experimental ——— and calculated ■) (c) (clay 1.0 g dm^{-3}, pH 4.0 and controlled temperature at 298±1 K).

from solution by the adsorbent indicated that the interaction between the metal ions and the adsorbent was an exchange process (Huheey *et al.*, 1993; Xia *et al.*, 1997; Salih *et al.*, 1998; Xu *et al.*, 2006; Sharma and Tomar, 2008; Sheng *et al.*, 2008). The reason for little sorption in acidic solution is the competition between the excess H^+ ions in the medium and other cationic species in solution. Greater acid concentrations suppress hydrolysis of the metal ions. In addition, as pH was increased, the positive surface charge decreased, resulting in less coulombic repulsion of the adsorbing metal ions (Sharma and Tomar, 2008).

Effect of contact time

For evolution of adsorption as a function of contact time, reaction intervals from 2.5 to 36 h were applied for all the matrices (Figure 7a,b), giving identical abrupt increases in adsorption for relatively small amounts of time before reaching the plateaux. According to the data, equilibrium was achieved at ~2, 3, and 4 h for Eu(III), U(VI), and Th(IV), respectively. For the maximum amount of radionuclides to be adsorbed, at high concentrations and over the shortest period of time possible, requires an excellent affinity of the adsorbents for these metals from the aqueous medium. In order to study the specific rate constant of the Th(IV)-/U(VI)-/Eu(III)-phyllosilicate systems, a Lagergren pseudo-second-order rate equation was used to simulate the kinetic adsorption of metals on the phyllosilicates. When the rate of an adsorption reaction was controlled by chemical exchange, a pseudo-second order model was better adjusted to the experimental kinetic data (Ho and McKay, 1999; Sheng *et al.*, 2008), as expressed by equation 6.

$$\frac{t}{N_f} = \left(\frac{1}{k_2 N_{fEQ}^2}\right) + \left(\frac{1}{N_{fEQ}}\right) t \qquad (6)$$

where k_2 is the pseudo-second order rate constant (mmol $g^{-1}min^{-1}$). The values of k_2 can be obtained from the non-linear regression plot of N_f *vs. t*. By carrying out a set of experiments at constant temperature and monitoring the amount adsorbed with time, the kinetics of the adsorption process can be determined. The values of k_2 and N_{fEQ} were obtained for M and M_{MTTZ} (Table 2). The correlation coefficient of the pseudo-second-order rate equation (r^2) for the non-linear regression was 0.999 for probability p = 0.0001, suggesting that the kinetic adsorption can be described very well by the pseudo-second-order rate equation. An example of a calculated curve obtained with non-linear regression for system M_{MTTZ}/Eu(III) (Karadag *et al.*, 2007; Guerra *et al.*, 2008b) is shown in Figure 7c.

Effect of metal concentration

M and M_{MTTZ} have been used to evaluate the maximum adsorption capacity for uptaking metal ions,

Table 2. Thermodynamic and kinetic data for radionuclides adsorption onto natural and modified magadiite samples (clay 1.0 g dm^{-3}, pH 4.0, time 8.0 h, and controlled temperature of 298±1 K).

Metal	N_f^{max} (10^{-3} mmol g^{-1})	N_s (10^{-3} mmol g^{-1})	$-\Delta h_{int}$ (J g^{-1})	$-\Delta H_{int}$ (kJ mol^{-1})	n	$K_S \times <10^{-3}$	r^2 (p = 1×10^{-4})	$-\Delta G_{int}$ (kJ mol^{-1})	$\Delta\Sigma_{int}$ (J $K^{-1}mol^{-1}$)	k_2 (10^{-3}mmol $g^{-1}min^{-1}$)	N_{fEQ} (10^{-3} mmol g^{-1})
M											
Th(IV)	1.5±0.1	1.97±0.1	8.33±1	4.25±2±0.1	0.71	8.2±2	0.999	22.3±2	60±1	18.7±0.1	1.85±0.2
U(VI)	1.6±0.1	2.60±0.2	13.39±2	5.13±0.2	0.79	12.2±1	0.998	23.3±1	61±3	20.1±0.2	2.13±0.1
Eu(III)	1.8±0.1	2.92±0.2	16.42±1	5.51±0.1	0.86	17.2±1	0.999	24.2±1	61±1	22.8±0.1	2.71±0.3
M_{MTTZ}											
Th(IV)	7.5±0.1	8.02±0.1	60.91±2	7.61±0.1	0.75	6.7±1	0.998	21.9±1	48±1	23.1±0.3	7.90±0.1
U(VI)	9.8±0.1	10.60±0.2	78.41±1	7.41±0.1	0.87	8.1± 1	0.999	22.3±1	50±1	26.2±0.1	10.20±0.1
Eu(III)	12.9±0.1	13.02±0.2	94.71± 2	7.32±0.1	0.95	10.4± 1	0.998	22.9±1	53±2	28.3± 0.2	13.01± 0.1

such as Th(IV), U(VI), and Eu(III), from aqueous solutions. The cations mentioned actually act as Lewis acid centers which interact with the nitrogen Lewis base centers attached to the pendant molecules covalently bonded to the modified clay surface and hydroxyl groups attached to the natural clay surface. Such processes occurring at the solid/liquid interface give the isotherms that demonstrate the saturation of the natural and modified clay samples with a definite number of moles of metallic cations (Figure 8a,b), with the most pronounced adsorption for Eu and a sample curve obtained with non-linear regression for the system M_{MTTZ}/Eu(III) (Karadag *et al.*, 2007; Guerra *et al.*, 2008b) (Figure 8c). Based on this ability of the pendant groups attached to the inorganic backbone to coordinate these metallic cations, the quantity can be related to N_f^{max}, which gave values of 7.5, 9.8, and 12.9×10^{-3} mmol g^{-1} for Th(IV), U(VI), and Eu(III), respectively (Table 2).

Thermodynamic study

A series of increments of 10 μL of metal solutions was added to the Th(IV)-/U(VI)-/Eu(III)-M/-M_{MTTZ} to elucidate the thermal interaction effect (Q_t). Two other titrations were needed to complete the experiment: (1) the thermal effect due to hydration of M and M_{MTTZ} (Q_h), which normally gives a null value; and (2) the dilution effect of metal solution in water, without a sample in the vessel (Q_d). The resulting thermal effect was given by the following equation: $\Sigma Q_r = \Sigma Q_t - \Sigma Q_d$ (Ruiz and Airoldi, 2004; Macedo *et al.*, 2007). Many investigations, in a variety of systems concerning the solvent effect on different matrices, have shown that this thermal effect is equal to zero (Prado and Airoldi, 2001; Ruiz and Airoldi, 2004; Lazarin and Airoldi, 2007; Guerra *et al.*, 2008a, 2008b).

The molar enthalpy (ΔH_{int}) of the process can be calculated by the expression $\Delta H_{int} = \Delta h_{int} N_S$. The Gibbs

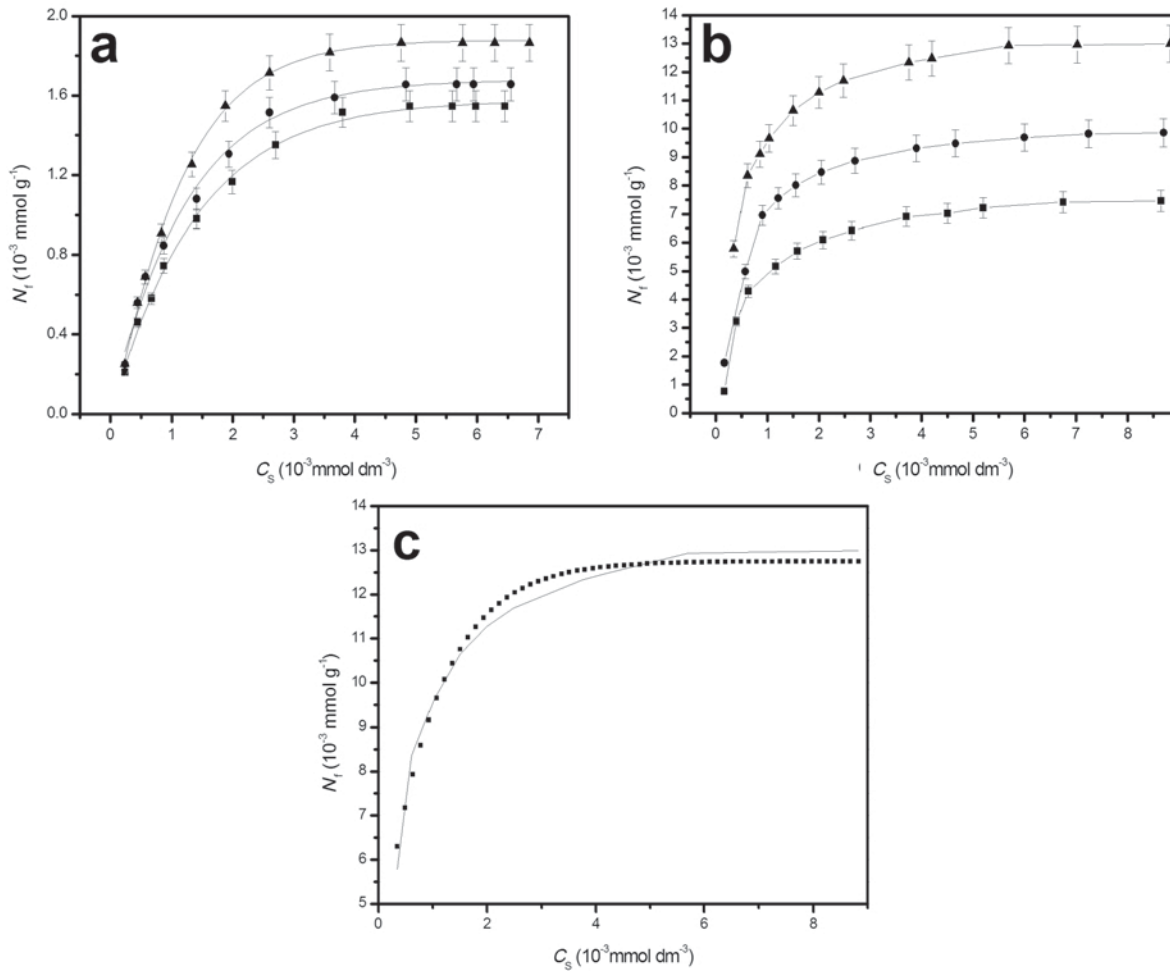

Figure 8. Adsorption of radionuclides onto natural (a) and modified (b) magadiite samples [■ – Th(IV), ● – U(VI), and ▲ – Eu(III)] and example of curve obtained by non-linear regression: M_{MTTZ}/Eu(III) (experimental ———; calculated ■) (c) (clay 1.0 g dm^{-3}, pH 4.0, time 8.0 h, and controlled temperature at 298±1 K).

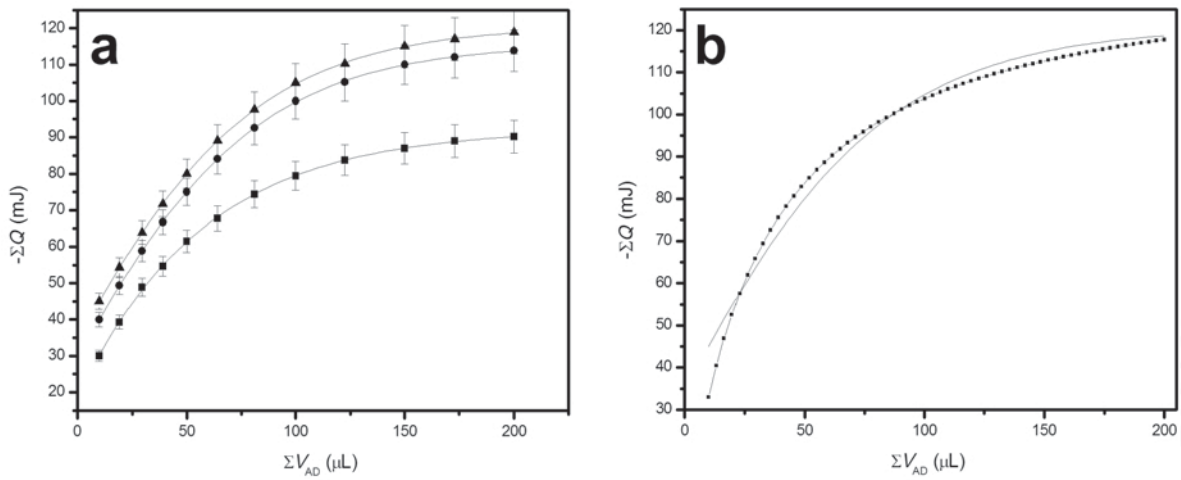

Figure 9. The resulting thermal effects of the adsorption isotherms for the radionuclides [■ – Th(IV), ● – U(VI), and ▲ – Eu(III)] (a) and example curve obtained by non-linear regression: M_{MTTZ}/Eu(III) (experimental ———; calculated ■) (b) (clay 1.0 g dm^{-3}, pH 4.0, and time 8.0 h).

free energy can be calculated by the equation $\Delta G_{int} = -RT \ln K_S$; finally, the entropy was calculated from $\Delta G_{int} = \Delta H_{int} - T\Delta S_{int}$ (Prado and Airoldi, 2001; Ruiz and Airoldi, 2004; Lazarin and Airoldi, 2007; Guerra *et al.*, 2008a, 2008b).

From calorimetric titration data, the net thermal effects resulted in the corresponding well behaved isotherms that were fitted to the Sips model (Figure 9a). The curve for Eu obtained with non-linear regression (Karadag *et al.*, 2007) is shown in Figure 9b. As an example, one of the titration thermograms obtained when M_{MTTZ} adsorbed the Eu(III) shows that, under the conditions applied, equilibrium was attained rapidly (Figure 10). The integrated heat value was obtained by use of the data treatment *Digitam* 4.1 program (Thermometric, Jarfalla, Sweden). Complete sets of thermodynamic data for each system studied are listed in Table 2. As observed, cation/basic center interactions for all systems were spontaneous in nature as reflected in their negative enthalpic values. The series of exothermic enthalpic data did not permit the distinguishing of a preference of any particular cation to bond with the available basic centers attached to the pendant groups covalently bonded to the inorganic backbone. However, the positive entropic values for all interactions that contribute to the favorable interactive process were associated with displacement of solvent molecules, initially bonded to the inorganic matrix, which was reinforced by desolvation of the cations before interacting with the basic centers. In such interactive processes the increase in free molecules in the reaction medium gave a positive entropy, thus demonstrating a favorable set of thermodynamic data for this kind of system (Prado and Airoldi, 2001; Machado *et al.*, 2004; Ruiz and Airoldi, 2004; Lazarin and Airoldi, 2007; Guerra *et al.*, 2008a, 2008b). An illustration of all the steps of the calorimetric titration of 0.020 g of original magadiite with 2.0×10^{-2} mmol dm^{-3} of Th(IV) solution is shown in Figure 11. The thermodynamic cycle for this series of adsorptions involving a suspension (susp) of magadiite samples (Mag_X) in aqueous (aq) solution with metallic cation (M^{4+}) can be represented by the following calorimetric reactions (equations 7–10):

$$Mag_{X(susp)} + M^{4+}_{(aq)} \rightarrow Mag_X...M^{4+}_{(susp)} \quad \Sigma Q_t \quad (7)$$
$$Mag_{X(susp)} + nH_2O \rightarrow Mag_X...nH_2O \quad \Sigma Q_h \quad (8)$$
$$M^{4+}_{(aq)} + nH_2O \rightarrow M^{4+}...nH_2O_{(aq)} \quad \Sigma Q_d \quad (9)$$
$$Mag_{X(susp)} + M^{4+}_{(aq)} \rightarrow Mag_X...M^{4+} \quad \Sigma Q_r \quad (10)$$

Regeneration of the adsorbents

Desorption and regeneration studies illustrate the nature of adsorption. Desorption experiments were

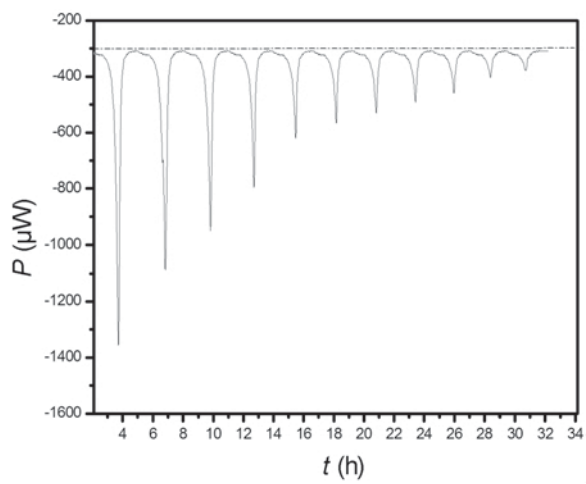

Figure 10. Variation of the thermal effect *vs.* time upon microcalorimetric titration of modified magadiite (M_{MTTZ}) suspended in water with 20.0 cm^3 of Eu(III) at 298±1 K conditions as specified in text.

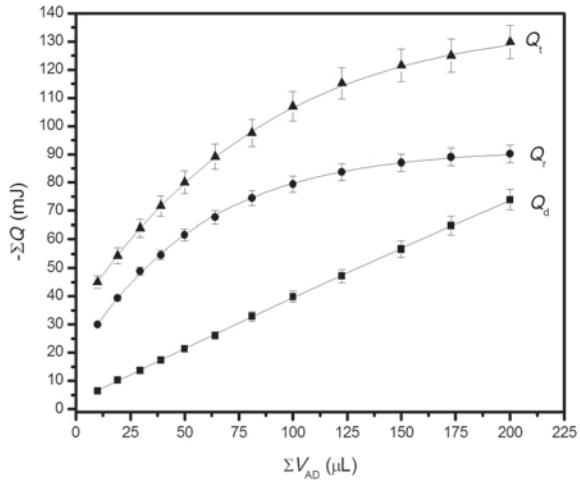

Figure 11. The resulting thermal effect of Th(IV) adsorption on modified magadiite at 298±1 K. The experimental points represent the thermal effect of cation titration ΣQ_t (▲), cation dilution ΣQ_d (■), and the net thermal interaction effect ΣQ_r (●); ΣQ and V_{ad} values are the sum of detected thermal effect and total injected volume of the Th(IV) solution.

carried out here in order to verify the mechanism of adsorption of Th(IV), U(VI), and Eu(III) on original and modified magadiite. Batch desorption studies were carried out by agitating 20.0 cm^3 of 100.0 mg dm^{-3} metallic ion solutions with 80.0 mg of M and M_{MTTZ} for 350 min. The remaining liquid phase was separated from the solid phase, and the metal-loaded adsorbents were firstly washed with deionized water (DDW) to remove non-adsorbed metallic ions. The metal-loaded adsorbents were then agitated with 20.0 cm^3 of aqueous solutions: 1.00 mol dm^{-3} (HCl), 1.00 mol dm^{-3} (HNO_3), and 0.50 mol dm^{-3} (NaOH) for up to 1 h. Investigations of the regeneration capacity indicated that NaOH did not promote any notable removal (<10.0%) of the metal ion-loaded adsorbents after 1 h of contact time. In addition, the best recovery results were achieved by using HCl (⩾94.0%) and HNO_3 (⩾97.0%), indicating that the metallic ions should interact with the pendant groups attached to the inorganic backbone of the magadiite. The regeneration of these materials makes possible their reutilization as adsorbents in subsequent adsorption cycles. The adsorption capacitiess of the regenerated materials were ~85.0% and 87.0% of the original absorbents, M and M_{MTTZ}, respectively, for Th(IV), U(VI), and Eu(III) (Figure 12a,b), indicating that the original and modified magadiite are good alternative adsorbents for removal of radionuclides from aqueous solutions.

CONCLUSIONS

Studies of metal adsorption onto raw and modified magadiite structures demonstrated that the natural and inorganic-organic materials can act as chelating agents in the removal of pollutant metal ions from aqueous solution; adsorption was in the following order: Eu(III) > U(VI) > Th(IV) considering pH, contact time, and metal concentration as variables. These results are in agreement with the affinity of the reactive basic center for cation coordination on the available pendant groups attached to the inorganic backbone. The quantitative metal/reactive center interactions for chemically modified magadiite clay were studied by means of calorimetric titration at the solid/liquid interface to give favorable sets of data such as exothermic enthalpy, negative Gibbs free energy, and positive entropic values. The thermodynamic data suggest the use of this series of synthetic, natural, and modified layered materials to improve the environment as cation-extraction agents.

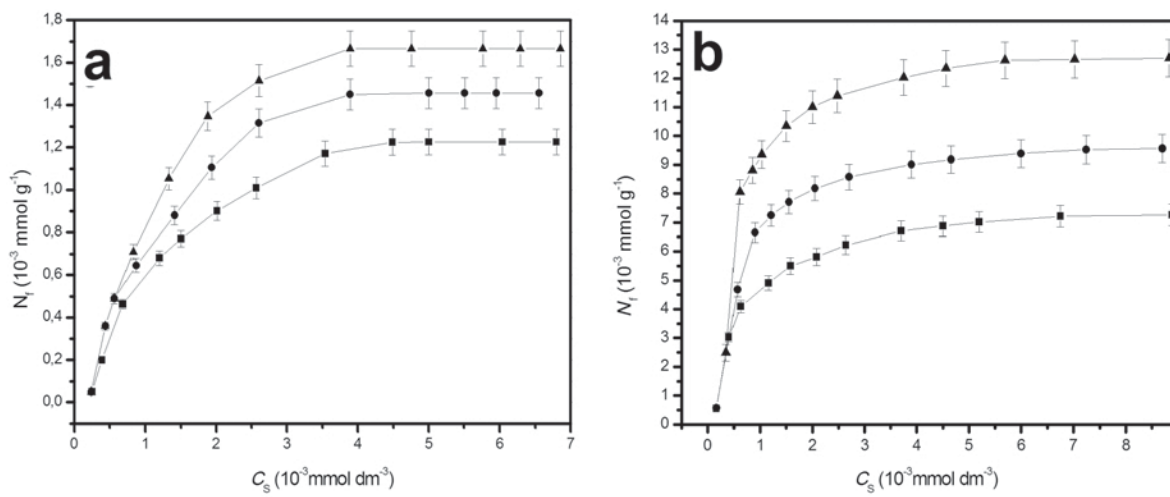

Figure 12. Adsorption of radionuclides onto regenerated adsorbents: original (a), and modified magadiite (b). ■ – Th(IV), ● – U(VI), and ▲ – Eu(III) (matrix 1.0 g dm^{-3}, pH 4.0, time 360 min, and controlled temperature at 298±1 K).

The data obtained suggest the possible industrial use of such materials in the removal of heavy elements from natural- as well as waste-water systems. The structural features of the new, synthesized materials with long chains suggest that it could be modified further, using other synthetic approaches, to yield higher-stage pendant chains, for a wide variety of chemical applications.

ACKNOWLEDGMENTS

The authors are indebted to CNPq for fellowships and to FAPESP for financial support.

REFERENCES

Alcântara, E.F.C., Faria, E.A., Rodrigues, D.V., Evangelista, S.M., DeOliveira, E., Zara, L.F., Rabelo, D., and Prado, A.G.S. (2007) Modification of silica gel by attachment of 2-mercaptobenzimidazole for use in removal Hg(II) from aqueous media: A thermodynamic approach. *Surface Science*, **311**, 1–7.

Almond, G.G., Harris, R.K., and Franklin, K.R. (1997) A structural consideration of kanemite, octosilicate, magadiite and kenyaite. *Journal of Materials Chemistry*, **7**, 681–687.

Babel, S. and Kurniawan, T.A. (2003) Low-cost adsorbents for heavy metals uptake from contaminated water: a review. *Journal of Hazardous Materials*, **97**, 219–243.

Barret, E.P., Joyner, L.G., and Halenda, P.P. (1951) The determination of pore volume and area distribution in porous substances. I. Computation from nitrogen isotherms. *Journal of the American Chemical Society*, **73**, 373–380.

Beurlen, H., Da Silva, M.R.R., Thomas, R., Soares, D.R., and Olivier, P. (2008) Nb-Ta-(Ti-Sn) oxide mineral chemistry as tracer of rare element granitic pegmatite fractionation in the Borborema Province, Northeastern Brazil. *Mineralium Deposita*, **43**, 207–228.

Brunauer, S., Emmett, P.H., and Teller E.E. (1938) The adsorption of gas in multimolecular layer. *Journal of the American Chemical Society*, **60**, 309–319.

Cestari, A.R., Vieira, E.F.S., Vieira, G.S., da Costa, L.P., Tavares, A.M.G., Loh, W., and Airoldi, C. (2009) The removal of reactive dyes from aqueous solutions using chemically modified mesoporous silica in the presence of anionic surfactant – The temperature dependence and a thermodynamic multivariate analysis. *Journal of Hazardous Materials*, **161**, 307–316.

Dias Filho, N.L. (1998) Adsorption of copper(II) and cobalt(II) complexes on a silica gel surface chemically modified with 3-amino-1,2,4-triazole. *Colloids and Surfaces, A. Physicochemical and Engineering Aspects*, **144**, 219–227.

Díaz, U., Cantín, A., and Corma, A. (2007) Novel layer organic-inorganic hybrid materials with bridged silsesquioxanes as pillars. *Chemistry of Materials*, **19**, 3686–3693.

Evangelista, S.H.M., De Oliveira, E., Castro, G.R., Zara, L.F., and Prado, A.G.S. (2007) Hexagonal mesoporous silica modified with 2-mercaptothiazoline for removing mercury from water solution. *Surface Science*, **601**, 2194–2202.

Fialips, C.I., Huo, D., Yan, L., Wu, J., and Stucki, J.W. (2002) Infrared study of reduced and reduced-reoxidized ferruginous smectite. *Clays and Clay Minerals*, **50**, 455–469.

Freundlich, H.M.F. (1906) Über die adsorption in Iösungen. *Zeitschrift für Physikalische Chemie* (Leipzig), **57A**, 385–470.

Garces, J.M., Rocke, S.C., Crowder, C.E., and Hasha, D.L. (1988) Hypothetical structures of magadiite and sodium octosilicate and structural relationships between the layered alkali metal silicates and the mordenite- and pentasil-group zeolites. *Clays and Clay Mnerals*, **36**, 409–418.

Guerra, D.L., Lemos, V.P., Airoldi, C., and Angélica, R.S. (2006) Influence of the acid activation of pillared smectites from Amazon (Brazil) in adsorption process with butilamine. *Polyhedron*, **25**, 2880–2890.

Guerra, D.L., Airoldi, C., Lemos, V.P., Angélica, R.S. and Viana, R.R. (2007) Aplicação de Al-PILC na adsorção de Cu^{2+}, Ni^{2+},Co^{2+} utilizando modelos físico-químicos de adsorção. *Eclética Química*, **32**, 51–60.

Guerra, D.L., Airoldi, C., Lemos, V.P., and Angélica, R.S. (2008a) Adsorptive, thermodynamic and kinetic performances of Al/Ti and Al/Zr-pillared clays from the Brazilian Amazon region for zinc cation removal. *Journal of Hazardous Materials*, **155**, 230–242.

Guerra, D.L., Airoldi, C., and Viana, R.R. (2008b) Performance of modified montmorillonite clay in mercury adsorption process and thermodynamic studies. *Inorganic Chemistry Communications*, **11**, 20–24.

Guo, Y., Wang, Y., Yang, Q.-X., Li, G.-D., Wang, C.-S, Cui, Z.-C., and Chen, J.-S. (2004) Preparation and characterization of magadiite grafted with an azobenzene derivative. *Solid State Sciences*, **6**, 1001–1006.

Ho, Y.S. and McKay, G.M. (1999) Pseudo-second order model for sorption process. *Process Biochemistry*, **34**, 451–465.

Huheey, J.E., Keiter, E.A., and Keiter, R.L. (1993) *Inorganic Chemistry, Principles of Structure and Reactivity*. Harper Collins, New York.

Jänchen, J., Morris, R.V., Bish, D.L., Janssen, M., and Hellwig, U. (2009) The H_2O and CO_2 adsorption properties of phyllosilicate-poor palagonitic dust and smectites under Martian environmental conditions. *Icarus*, **200**, 463–467.

Karadag, D., Koc, Y., Turan, M., and Ozturk, M. (2007) A comparative study of linear and non-linear regression analysis for ammonium exchange by clinoptilolite zeolites. *Journal of Hazardous Materials*, **144**, 432–437.

Komori, Y., Miyoshu, M., Hayashi, S., Sugahara, Y., and Kuroda, K. (2000) Characterization of silanol groups in protonated magadiite by 1H and 2H solid-state nuclear magnetic resonance. *Clays and Clay Minerals*, **48**, 632–637.

Lagergren, S. (1898) About the theory of so-called adsorption of soluble substances. *Kungliga Suenk Vetenskapsakademiens Handlingar*, **241**, 1–39.

Langmuir, I. (1918) The adsorption of gases on plane surfaces of glass, mica and platinum. *Journal of the American Chemical Society*, **40**, 1361–1403.

Lazarin, A.M. and Airoldi, C. (2007) Thermochemistry of intercalation of n-alkylmonoamines into lamellar hydrated barium phenylarsonate. *Thermochimica Acta*, **454**, 43–49.

Leppert, D. (1990) Heavy metal sorption with clinoptilolite zeolite: alternatives for treating contaminated soil and water. *Mining Engineering*, **42**, 604–608.

Macedo, T.R., Petrucelli, G.C., and Airoldi, C. (2007) Silicic acid magadiite guest molecules and features related to the thermodynamics of intercalation. *Clays and Clay Minerals*, **55**, 151–159.

Machado, T.R., Fonseca, M.G., Arakaki, L.N.H., and Oliveira, S.F. (2004) Silica gel containing sulfur, nitrogen and oxygen as adsorbents centers on surface for removing copper from aqueous/ethanolic solutions. *Talanta*, **63**, 317–322.

Malkoc, E., Nuhoglu, Y., and Dundar, M. (2006) Adsorption of chromium(VI) on pomace – an olive oil industry waste: batch and column studies. *Journal of Hazardous Materials*, **138**, 142–151.

Mizukami, N., Mizukami, N., Tsujimura, M., Kuroda, K., and Ogawa, M. (2002) Preparation and characterization of Eu-magadiite intercalation compounds. *Clays and Clay Minerals*, **50**, 799–806.

Pérez-Quintanilla, D.P., Del Hierro, I., Fajardo, M., and Serra, I (2007) Preparation, characterization, and Zn^{2+} adsorption behavior of chemically modified MCM-41 with 5-mercapto-

1-methyltetrazole. *Journal of Colloid and Interface Science*, **313**, 551–562.

Pérez-Quintanilla, D.P., Del Hierro, I., Fajardo, M., and Serra, I. (2006) 2-Mercaptothiazoline modified mesoporous silica for mercury removal from aqueous media. *Journal of Hazardous Materials*, **134**, 245–256.

Prado, A.G.S. and Airoldi, C. (2001) Adsorption preconcentration and separation of cations on silica gel chemically modified with the herbicide 2,4-dichlorophenoxyacetic acid. *Analytica Chimica Acta*, **432**, 201–211.

Ruiz, V.S.O. and Airoldi, C. (2004) Thermochemical data for n-alkylmonoamine intercalation into crystalline lamellar zirconium phenylphosphonate. *Thermochimica Acta*, **420**, 73–78.

Salih, B., Denizli, A., Kavakli, C., and Pişkin, E. (1998) Adsorption of heavy metal ions onto dithizone-anchored poly (EGDMA-HEMA) microbeads. *Talanta*, **46**, 1205–1213.

Shahwan, T. and Erten, H.N. (2005) Characterization of Sr^{2+} uptake on natural minerals of kaolinite and magnesite using XRPD, SEM/EDS, XPS, and DRIFT. *Radiochimica Acta*, **93**, 225–232.

Shanmugharaj, A.M., Rhee, K.Y., and Ryu, S.H. (2006) Influence of dispersing medium on grafting of aminopropyltriethoxysilane in swelling clay materials. *Journal of Colloid and Interface Science*, **298**, 854–859.

Sharma, P. and Tomar, R. (2008) Synthesis and application of an analogue of mesolite for removal of uranium(VI), thorium(IV), and europium(III) from aqueous waste. *Microporous and Mesoporous Materials*, **116**, 641–652.

Sheng, G., Hu, J., and Wang, X. (2008) Sorption properties of Th(IV) on the raw diatomite – Effects of contact time, pH, ionic strength and temperature. *Applied Radiation and Isotopes*, **66**, 1313–1320.

Sips, R. (1948) On the structure of a catalyst surface. *Journal of Chemical Physics*, **16**, 490–495.

Stucki, J.W., Wu, J., Gan, H., Komadel, P., and Banin A. (2000) Effect of iron oxidation state and organic cations on dioctahedral smectite hydration. *Clays and Clay Minerals*, **48**, 290–298.

Tang, X., Li, Z., and Chen, Y. (2009) Adsorption behavior of Zn(II) on calcinated Chinese loess. *Journal of Hazardous Materials*, **161**, 824–834.

Xia, K., Bleam, W., and Helmke, P.A. (1997) Studies of the nature of binding sites of first row transition elements bound to aquatic and soil humic substances using X-ray absorption spectroscopy. *Geochimica et Cosmochimica Acta*, **61**, 2223–2235.

Xiu-Wen, W., Hong-Wen, M., Jin-Hong, L., Zhang, J., and Zhi-Hong, L. (2007) The synthesis of mesoporous aluminosilicate using microcline for adsorption of mercury(II). *Journal of Colloid and Interface Science*, **315**, 555–561.

Xu, D., Wang, K.X., Chen, C.L., Zhou, X., and Tan, X.L. (2006) Influence of soil humic acid and fulvic acid on sorption of Thorium(IV) on MX-80 bentonite. *Radiochimica Acta*, **94**, 429–434.

(*Received 25 April 2009; revised 5 November 2009; Ms. 312; A.E. J.D. Fabris*)